MedChemComm

RESEARCH ARTICLE

View Article Online
View Journal | View Issue

Cite this: *Med. Chem. Commun.*, 2018, **9**, 2055

Development of selective, fluorescent cannabinoid type 2 receptor ligands based on a 1,8-naphthyridin-2-(1*H*)-one-3-carboxamide scaffold†

Anna G. Cooper,[a] Caitlin R. M. Oyagawa,[b] Jamie J. Manning,[b] Sameek Singh,[a] Sarah Hook,[a] Natasha L. Grimsey,[b] Michelle Glass,[b] Joel D. A. Tyndall[a] and Andrea J. Vernall*[a]

Received 7th September 2018,
Accepted 18th October 2018

DOI: 10.1039/c8md00448j

rsc.li/medchemcomm

Cannabinoid type 2 (CB_2) receptor has been implicated in several diseases and conditions, however no CB_2 receptor selective drugs have made it to market. The aim of this study was to develop fluorescent ligands as CB_2 receptor tools, to enable an increased understanding of CB_2 receptor expression and signalling and thereby accelerate drug discovery. Fluorescent ligands have been successfully developed for other receptors, however none with adequate subtype selectivity or imaging properties have been reported for CB_2 receptor. A series of 1,8-naphthyridin-2-(1*H*)-one-3-carboxamides with linkers and fluorophores appended in the N1 and C3-positions were developed. Molecular modelling indicated the C3 *cis*-cyclohexanol-linked compounds directed the linker out of the CB_2 receptor between transmembrane helices 1 and 7. Herein we report fluorescent ligand **32** (hCB_2 pK_i = 6.33 ± 0.02) as one of the highest affinity, selective CB_2 receptor fluorescent ligands reported. Despite **32** displaying poor specific labelling of CB_2 receptor, the naphthyridine scaffold with this linker remains highly promising for future development of CB_2 receptor tools.

Introduction

Cannabinoid type 2 (CB_2) receptor is a class A G protein-coupled receptor (GPCR) and is highly expressed in immune cells and lymphoid tissues,[1] and in lower levels in the central nervous system.[2] Along with cannabinoid type 1 (CB_1) receptor, the endogenous agonists anandamide and 2-arachidonoylglycerol and various regulatory enzymes, CB_2 receptor is part of the highly regulated endocannabinoid system.[3] CB_2 receptor modulates cytokine release and immune cell migration, thereby regulating immune responses and inflammatory pathways.[4,5] CB_2 receptor has been shown to play a role in neurodegenerative disorders,[6] pain,[7] atherosclerosis[8] and cancer.[9] As such, ligands of CB_2 receptor hold promise as therapeutic interventions. However, to date no CB_2 receptor selective drugs have made it to market, though a few have undergone clinical trials.[10] Drug development efforts would be greatly aided by an increased understanding of CB_2 receptor expression and signalling. The aim of this study was therefore to develop high affinity, selective CB_2 receptor fluorescent ligands and evaluate these ligands as imaging tools. Fluorescent ligands have been successfully developed for other Class A GPCRs[11] and used, for example, to visualise receptor,[12] track receptor internalisation[13,14] and to study single-cell ligand binding kinetics.[15]

In order to be useful imaging tools, fluorescent GPCR ligands require high affinity and selectivity, and should exhibit low levels of non-specific membrane interactions. A typical strategy for developing fluorescent ligands is to select a known high affinity and selective ligand as a scaffold to which a linker and fluorophore can be appended. It is crucial to identify a suitable position on the scaffold for linker attachment in order to retain affinity for the target receptor and minimise disruption of the binding orientation of the pharmacophore.[11] It is particularly challenging to develop fluorescent ligands with minimal plasma membrane interactions for cannabinoid (CB) receptors due to the typically lipophilic nature of CB ligands.

There have been several reports of fluorescent ligands for CB_2 receptor, however, these lack either receptor subtype selectivity or display high levels of non-specific binding/interactions rendering these ligands unsuitable for use in techniques such as confocal microscopy.[16–21] A scaffold based on SR144528 (Fig. 1) termed 'mbc94' has most commonly been utilised for development of CB_2 receptor fluorescent

[a] *School of Pharmacy, University of Otago, 18 Frederick Street, Dunedin 9054, New Zealand. E-mail: andrea.vernall@otago.ac.nz; Tel: +64 3 479 4518*
[b] *Department of Pharmacology and Clinical Pharmacology, and Centre for Brain Research, School of Medical Sciences, University of Auckland, Auckland, New Zealand*

† Electronic supplementary information (ESI) available. See DOI: 10.1039/c8md00448j

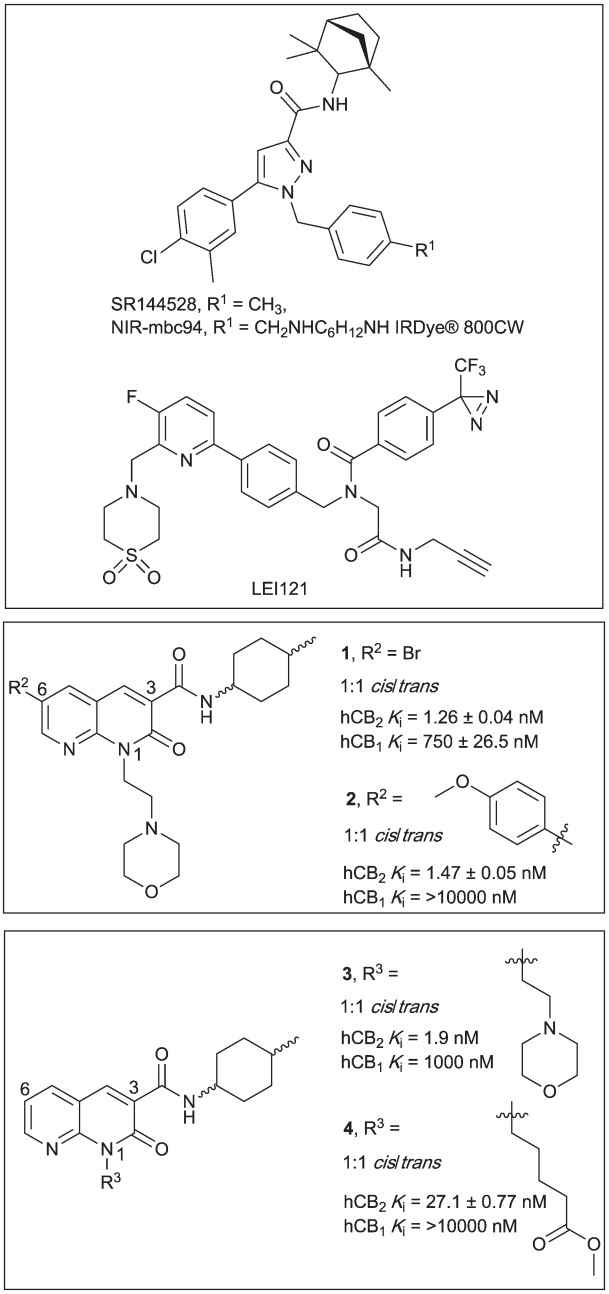

Fig. 1 Diarylpyrazole SR144528, and 1,8-naphthyridin-2-(1*H*)-one-3-carboxamides **1**–**4**, with previously reported binding affinities.[25]

ligands, for example NIR-mbc94 (Fig. 1, mCB$_2$ receptor K_i = 260 nM).[18] Fluorescent ligands based on an aminoalkylindole scaffold have also been attempted, however despite the ligand-linker conjugates retaining CB receptor affinity the fluorescent conjugates showed little CB receptor binding.[22,23] The bifunctional, photoreactive scaffold LEI121 (Fig. 1) has recently been reported as an alternative strategy to a 'pre-assembled' CB$_2$ receptor fluorescent ligand. Upon photo-activation, non-fluorescent LEI121 covalently bound to CB$_2$ receptor, which was then labelled *via* reaction of an azide-fluorophore to the alkyne of LEI121.[24] This is a promising strategy for interrogating CB$_2$ receptor, however a 'pre-assembled' non-covalent fluorescent ligand is still very desirable for many competition-based and kinetic experiments.

In this paper we report the development of CB$_2$ receptor fluorescent ligands based on the 1,8-naphthyridin-2-(1*H*)-one-3-carboxamide scaffold. Many derivatives of this scaffold are reported to have very high affinity and subtype selectivity for CB$_2$ receptor, (*e.g.* **1** and **4**,[25] Fig. 1) and there are structure–activity-relationships (SAR) reporting the effect of substitution at N1, C3 and C6 (ref. 26–29) (*e.g.* **1**–**4**,[25] Fig. 1). Additionally, the 1,8-naphthyridin-2-(1*H*)-one-3-carboxamide scaffold was selected because it is less lipophilic than many other cannabinoids (*e.g.* clog*P* of **2** is 2.93 compared to SR144528 clog*P* of 7.13), which is beneficial in terms of reducing the overall lipophilicity of a fluorescent ligand.

The N1, C3 and C6 naphthyridine positions were considered for linker and fluorophore attachment because there is SAR reported for these positions and all are synthetically accessible. Since SAR indicated groups of varying length and bulk were tolerated in the N1-position,[25,29] including a 'linker-like' methyl valerate (**4**, Fig. 1), one series of conjugates were developed linked at this position. A range of factors were considered when analysing if the C3 cyclohexyl carboxamide position might be amenable to linker and fluorophore attachment. The stereochemistry of the 4-methylcyclohexyl moiety at the C3 carboxamide has been shown to be influential on CB$_2$ receptor binding, with *cis* derivatives showing improved receptor affinity compared to *trans* derivatives.[25,27] This sensitivity of the methylcyclohexyl group could translate to a position not tolerant of much chemical change/variation, however ligand docking of **1** into a CB$_2$ receptor homology model (as is discussed for **28** in Modelling section) positioned the cyclohexyl group close to exiting CB$_2$ receptor between transmembrane helix (TMH) 1 and TMH7. This therefore made the C3 cyclohexyl carboxamide an appealing linker attachment position, especially in light of previously reported molecular dynamics simulations indicating that cannabinoids may enter into CB receptors *via* the lipid membrane between TMH6 and TMH7 or between TMH1 and TMH7.[30–32] Cyclohexanol and cyclohexylamine derivatives were designed to allow linker extension and both *cis* and *trans* isomers (of the cyclohexanol) were prepared since the previously established methylcyclohexyl *cis*/*trans* SAR could not be assumed to be the same.

The C6 position was not selected for linker attachment based on SAR that showed that functional activity can be controlled by the C6 substituent. For example, compound **3** (Fig. 1) behaved as a CB$_2$ receptor agonist in β-arrestin 2 and cAMP assays while **1** and **2** (Fig. 1) behaved as antagonists/inverse agonists in a β-arrestin 2 assay.[25] It has been postulated with docking studies that this C6 substituent orientates deep into a receptor binding pocket and modulates a CWFP flexible hinge motif on TMH6.[25] Linker substitution at C6 was therefore deemed most likely non-tolerable and likely would be detrimental to ligand affinity for CB$_2$ receptor. This was also the reason that the two fluorescent ligand series (N1-linked and C3-linked) were therefore developed with a small

C6 substituent present since the goal was to develop high affinity, CB_2 receptor selective fluorescent ligands that do not activate CB_2 receptor.

Results and discussion

Synthetic chemistry

The N1-linked series was assembled as a 1 : 1 *cis*/*trans* mix at the C3 cyclohexyl carboxamide as the first goal was to determine if the N1-position was tolerant of linker and fluorophore attachment. Commercially available 2-amino-3-pyridinecarboxaldehyde was converted to **5** in 3 steps following previously reported syntheses.[25] Alkylation of **5** with 4-(2-chloroethyl)morpholine hydrochloride afforded the previously reported **1** (ref. 25) (Scheme 1), which was used as a pharmacological control. Alkylation of **5** with methyl 5-bromovalerate or methyl 4-bromomethylbenzoate gave **6** or **7** in low yield, due to incomplete conversion of **5** and challenging separation of products from unreacted **5**. Both **6** and **7** are amenable to linker extension following methyl ester deprotection, however it was decided to proceed with valerate linked-**6** and only synthesise further benzoyl derivatives if **7** showed high affinity for CB_2 receptor. Bromo-**6** was subjected to Suzuki coupling with 4-methoxyphenylboronic acid to afford **8**, to enable comparison of the C6 bromo to methoxyphenyl substituent.

To further extend the distance of the naphthyridine core from the fluorophore the methyl ester of **6** underwent saponification to reveal carboxylic acid **9**, which was coupled to either *N*-Boc-1,8-octanediamine or *N*-Boc-2,2′-(ethylenedioxy)-diethylamine to yield **10** and **11** respectively. These alkyl and short PEG-like linkers of the same atom length were chosen as a way to compare different linker lipophilicity, since it was hypothesised that the lipophilic alkyl linker may be preferable for CB_2 receptor affinity, whereas the PEG-like linker may impart more hydrophilicty (than the equivalent alkyl linker) to the overall fluorescent ligand and lead to better imaging properties (*e.g.* lower non-receptor specific membrane

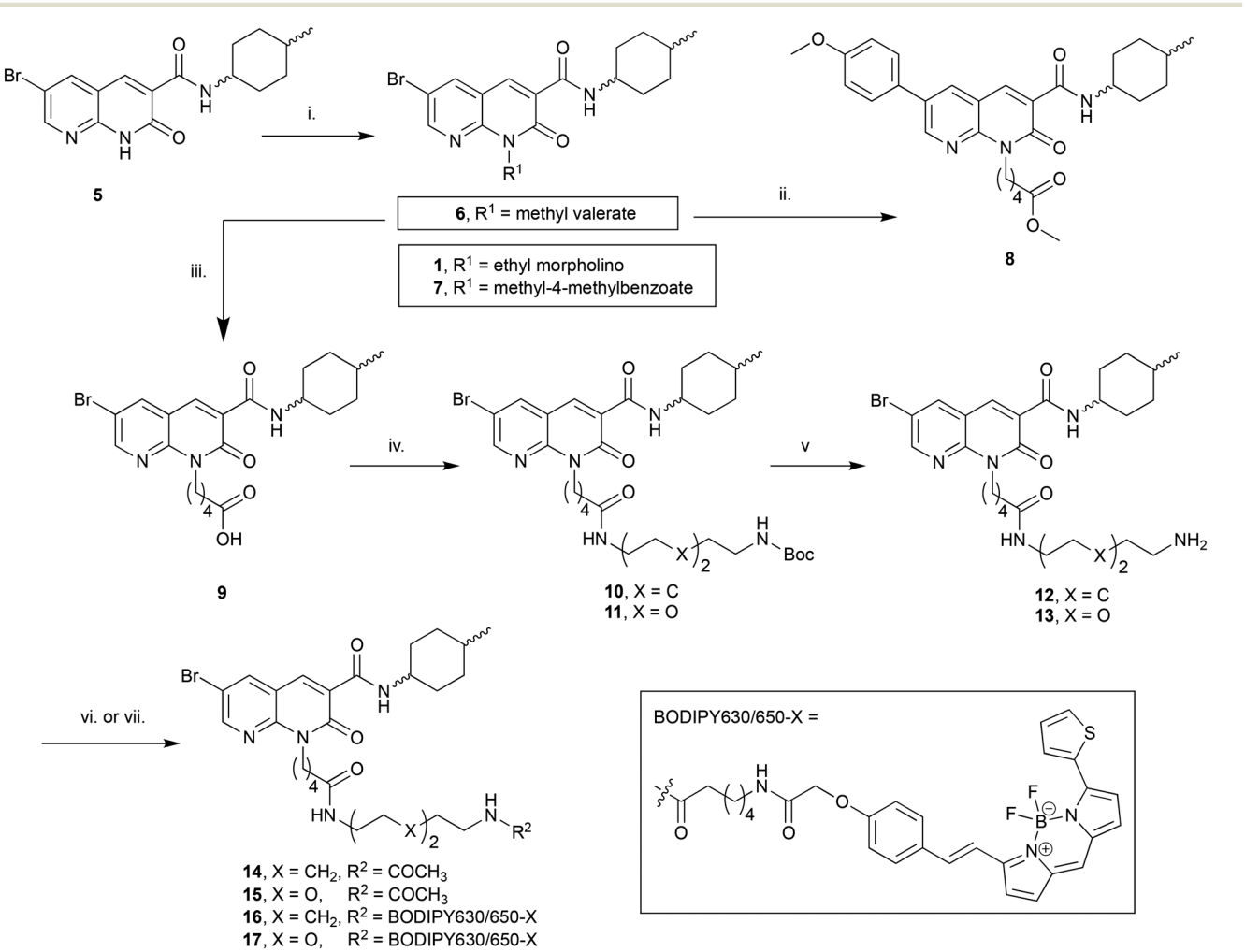

Scheme 1 Reagents and conditions: (i) 4-(2-Chloroethyl)morpholine hydrochloride, methyl 5-bromovalerate, or methyl 4-bromomethylbenzoate, Cs_2CO_3, DMF, 50 °C, 12 h, 22–37%; (ii) 4-methoxyphenylboronic acid, $Pd(OAc)_2$, Na_2CO_3, H_2O : DMF 1 : 4 v:v, 110 °C, 3 h, 55%; (iii) 10% aq. NaOH, EtOH, 110 °C, 5 h, 43%; (iv) *N*-Boc-1,8-octanediamine or *N*-Boc-2,2′-(ethylenedioxy)diethylamine, DIPEA, HATU, DMF, rt, 14 h, 71–77%; (v) TFA, DCM, rt, 1 h, 86–91%; (vi) Ac_2O, DIPEA, DCM, rt, 1 h, 95–96%; (vii) BODIPY 630/650-X-OSu, DIPEA, DMF, rt, 15 h, 88–92%. Compounds 1 : 1 *cis*/*trans*.

interactions). Boc deprotection of **10** and **11** yielded unprotected amines **12** and **13**, which were then each acetylated using acetic anhydride to give **14** and **15**. In a separate procedure these were reacted with 6-(((4,4-difluoro-5-(2-thienyl)-4-bora-3a,4a-diaza-sindacene-3-yl)styryloxy) acetyl) aminohexanoic acid, succinimidyl ester (BODIPY630/650-X-OSu) to yield fluorescent ligands **16** and **17**. The BODIPY630/650-X fluorophore has been used successfully to develop fluorescent ligands for other Class A GPCRs,[14,33,34] and has favourable properties (such as a good quantum yield, intense absorption and high chemical and photo stability) and as a red emitting fluorophore there is minimal detection interference from cellular autofluorescence.[35] A red-shifted fluorescent ligand also allows co-localisation experiments with, for example, green-fluorescent-protein-tagged receptors or proteins, to be carried out.

The C3-linked series was assembled in a different order to allow for more efficient variation of the C3 substituent. The previously reported **18** (ref. 25) was N1-alkylated, substituted at C6 with methoxyphenyl and the methyl ester saponified to afford **19** (Scheme 2). Carboxylic acid **19** was coupled in separate reactions to *cis*- or *trans*-4-aminocyclohexanol to give alcohols **20** and **21** respectively, or to 1-*N*-Boc-*cis*-1,4-cyclohexyldiamine to give *cis*-Boc-protected amine **22**.

The intention was to introduce an ether linkage *via* alkylation of alcohols **20** and **21**. However, despite several attempts using alkyl bromides such as *tert*-butyl bromoacetate or 2-(Boc)-amino-ethylbromide with either NaH or $CsCO_3$ as the base, varying equivalents of each base and addition order, and varying temperature the intended ether product was either detected only in trace amounts or not at all. An alternative synthetic strategy was envisaged, whereby the ether bond to the cyclohexyl could instead be preassembled and then coupled to **19**. Attempts to alkylate carboxybenzyl and dibenzyl protected 4-aminocyclohexanol with various alkyl bromides using a range of bases (NaH, $CsCO_3$, K_2CO_3, tBuOK and lithium bis(trimethylsilyl)amide), temperatures, solvents and reaction times were all unsuccessful. A Mitsunobu reaction to form the ether bond was not attempted due to the calculated pK_a (~15) of the cyclohexanol alcohol.

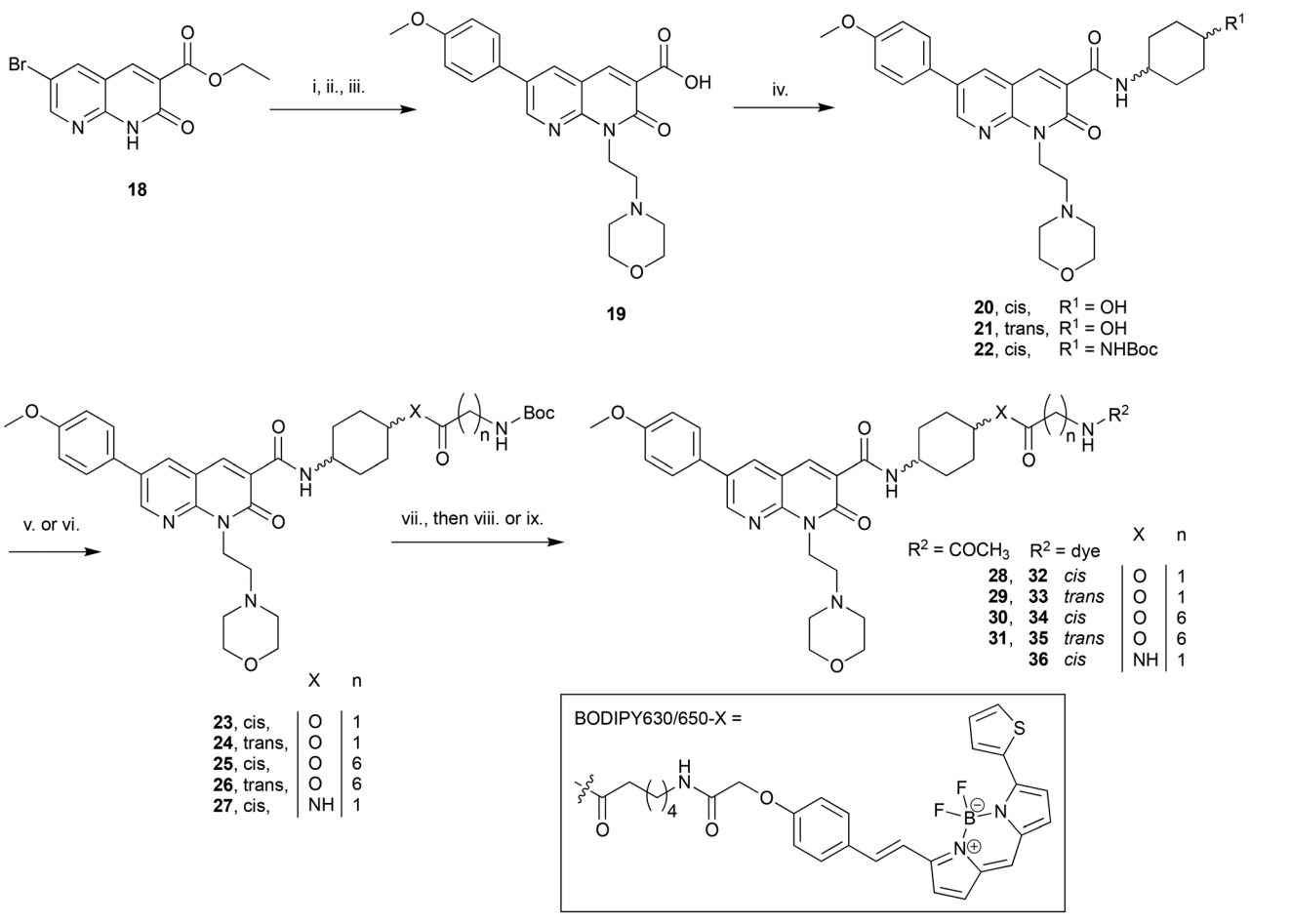

Scheme 2 Reagents and conditions: (i) 4-(2-Chloroethyl)morpholine hydrochloride, Cs_2CO_3, DMF, 50 °C, 12 h; (ii) 4-methoxyphenylboronic acid, Na_2CO_3, $Pd(OAc)_2$, H_2O, DMF, 110 °C, 3 h; (iii) 0.2 M aq. LiOH·H_2O, THF, 0 °C, 1 h, 20% over three steps; (iv) *cis*-4-aminocyclohexanol or *trans*-4-aminocyclohexanol or 1-*N*-Boc-*cis*-1,4-cyclohexyldiamine, HATU, DIPEA, DMF, rt, 14 h, 79–82%; (v) *N*-Boc-glycine or *N*-Boc-7-aminoheptanoic acid, TFFH, Et_3N, DMAP, DCM, rt, 14 h, 19–80%; (vi) 1.Trifluoroacetic acid (TFA), DCM, rt, 1 h, quantitative; 2. *N*-Boc-glycine, HATU, DIPEA, DMF, rt, 14 h, 31%; (vii) TFA, DCM, rt, 1 h, 45–57%; (viii) Ac_2O, DIPEA, DCM, rt, 1 h, 96–98%; (ix) BODIPY 630/650-X-OSu, DIPEA, DMF, rt, 14 h, 72–97%.

Since **20** and **21** were already prepared it was decided to proceed with formation of an ester bond to enable pharmacological evaluation of the C3-cyclohexyl-linker position, which could then be revisited for a more stable bond if the C3-position proved suitable. Activation of Boc-glycine or *N*-Boc-7-aminoheptanoic acid with tetramethylfluoroformamidinium hexafluorophosphate (TFFH) followed by addition of **20** or **21** yielded esters **23–26**. TFFH was used rather than a carbodiimide reagent in an attempt to counteract the poor nucleophilicity of alcohols **20** and **21**. Instead of using linkers analogous to the alkyl and PEG-like linkers of the *N*-substituted series, it was decided to use a commercially available single 'glycine' and a longer 7-aminoheptanoic acid linker to allow exploration of how varying linker length might effect receptor affinity. Boc-deprotection of **22** followed by HATU-mediated coupling of Boc-glycine afforded **27**, the analogous compound to **23** but with an amide replacing the ester bond. Boc-deprotection of **23–27** followed by either acylation or reaction with BODIPY630/650-X-OSu gave **28–31** or **32–36** respectively.

Pharmacology

A radioligand competition binding screen was carried out to determine the ability of 10 μM of **1**, **6–8**, **14–17**, **20**, **21**, **28–36** to displace [^{3}H]CP-55 940 (2.5 nM or 1 nM) from CB_2 or CB_1 receptor (data not shown). Compounds that displaced [^{3}H]CP55 940 by more than 50% were then evaluated at varying concentrations to determine pK_i values (Tables 1 and 2). Compounds with pK_i > 5 at CB_2 receptor were also analysed for function at CB_2 and CB_1 receptors in a cAMP assay (Tables 1 and 2).

N1-linked naphthyridines. The N1-linked naphthyridine with the highest affinity for CB_2 receptor (Table 1) was the previously reported *N*-ethyl morpholino **1**. In our hands, **1** had a pK_i of 7.26 ± 0.04, which was equivalent to that measured for SR144528 (pK_i 7.29 ± 0.03). This was a slightly different result to that previously reported wherein **1** had a ~0.5 log unit lower affinity than SR144528 in their study (Fig. 1 and ref. 25). Exchange of the ethyl morpholino group (**1**) with a methyl benzoate (**7**) greatly reduced CB_2 receptor binding, which was somewhat surprising since there are literature reports of similar naphthyridine scaffolds with N1-aromatic groups such as benzyl and *p*-fluorobenzyl with nanomolar CB_2 receptor affinity.[25,27] The affinities of N1-valerate linked **6** and **8** for CB_2 receptor were both poorer than the previously reported N1-valerate **4** (Fig. 1),[25] although **4** is unsubstituted at the C6 position. Unfortunately, extension of the N1-linker (**14**, **15**) and attachment of the BODIPY 630/650 fluorophore to this extended linker resulted in little affinity for CB_2 receptor. N1-linked **1**, **6–8** and **14–17** were also tested for CB_1 receptor affinity and, in agreement with previously reported naphthyridine compounds, none showed appreciable binding.

Table 1 Affinity and functional data of N1-linked naphthyridines

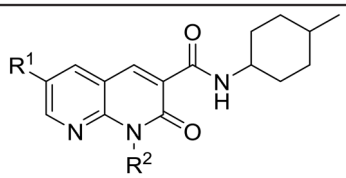

			CB_2 receptor			CB_1 receptor			
	R^1	R^2	pK_i[a] (±SEM)	pIC_{50}[b,c] (±SEM)	E_{max}[b,d] (% ± SEM)	pK_i (±SEM)[a]	pIC_{50} (±SEM)[b,c]	E_{max}[b,d] (% ± SEM)	CB_2 selectivity[e]
1	Br	Ethyl morpholino	7.26 ± 0.04	7.41 ± 0.17	166 ± 5.6	<5	No response[g]	89 ± 5.6[g]	>182
6	Br	$(CH_2)_4CO_2Me$	5.96 ± 0.04	6.24 ± 0.05[f]	161 ± 5.0[f]	<5	5.73 ± 0.14	134 ± 4.4	>9
7	Br	Methyl-4-methylbenzoate	<5	—	—	<5	—	—	—
8	Me-OPh	$(CH_2)_4CO_2Me$	6.59 ± 0.05	7.19 ± 0.27	139 ± 4.2	5.06 ± 0.03	6.02 ± 0.25	126 ± 3.2	33
14	Br	$(CH_2)_4CO$ $NH(CH_2)_8NHAc$	<5	—	—	<5	—	—	—
15	Br	$(CH_2)_4CO$ $NH(C_2H_4O)_2NHAc$	<5	—	—	<5	—	—	—
16	Br	$(CH_2)_4CO$ $NH(CH_2)_8NH$-BODIPY-630/650-X	<5	—	—	<5	—	—	—
17	Br	$(CH_2)_4CO$ $NH(C_2H_4O)_2NH$-BODIPY-630/650-X	<5	—	—	<5	—	—	—
SR144528		—	7.29 ± 0.03	6.90 ± 0.08	153 ± 3.8	5.40 ± 0.2	No response[g]	108 ± 3.6[g]	78

[a] Radioligand binding performed with [^{3}H]CP55 940 (2.5 nM) and HEK293-hCB_2 or -hCB_1 membranes. Data is the mean ± SEM of at least three individual experiments performed in triplicate. Compounds which at 10 μM significantly displaced [^{3}H]CP55 940 but with <50% displacement are annotated as having pK_i >5 M. [b] cAMP levels measured in a BRET assay using a CAMYEL biosensor, in either HEK-293-hCB_2 or hCB_1 cells. Data is the mean ± SEM of at least three independent experiments conducted in duplicate. [c] pIC_{50} calculated by concentration response. [d] E_{max} response (at 10 μM for compounds without pIC_{50} determined), normalised to basal (0%) and forskolin only (100%) levels of cAMP. E_{max} >100% is consistent with inverse agonism. [e] CB_2 receptor selectivity is calculated by: 10^(pK_i CB_2–pK_i CB_1) Naphthyridine compounds all 1 : 1 *cis*:*trans* mixture. [f] Except (**6**) which is two independent experiments performed in duplicate. '—' Indicates that pIC_{50} or E_{max} was not determined. [g] Indicates no significant difference from forskolin only (100%), indicating no measurable response.

Table 2 Affinity and functional data of cyclohexyl-linked naphthyridines

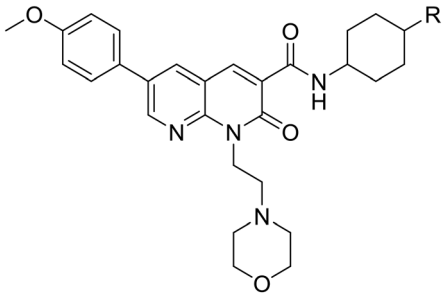

			CB_2 receptor			CB_1 receptor			
		R	pK_i[a] (±SEM)	pIC_{50}[b,c] (±SEM)	E_{max}[b,d] (% ± SEM)	pK_i[a] (± SEM)	pIC_{50}[b,c] (±SEM)	E_{max}[b,d] (% ± SEM)	CB_2 selectivity[e]
20	*cis*	OH	5.66 ± 0.07	6.74 ± 0.16	156 ± 5.5	<5	—	117 ± 2.4[f]	>4
21	*trans*	OH	5.47 ± 0.10	—	—	No binding	—	—	—
28	*cis*	$OC(O)CH_2NHAc$	5.99 ± 0.03	6.99 ± 0.11	154 ± 5.4	<5	No response[g]	115 ± 6.5[f,g]	>9
29	*trans*	$OC(O)CH_2NHAc$	<5	—	—	No binding	—	—	—
30	*cis*	$OC(O)C_6H_{12}NHAc$	5.51 ± 0.02	5.81 ± 0.15	179 ± 12.1	<5	—	130 ± 2.6[f]	>3
31	*trans*	$OC(O)C_6H_{12}NHAc$	5.43 ± 0.06	—	—	<5	—	—	>2
32	*cis*	$OC(O)CH_2NH$-BODIPY630/650-X	6.33 ± 0.02	6.72 ± 0.18	210 ± 15.7	<5	—	117 ± 3.5[h]	>21
33	*trans*	$OC(O)CH_2NH$-BODIPY630/650-X	5.23 ± 0.06	—	—	<5	—	—[g]	>1.6
34	*cis*	$OC(O)C_6H_{12}NH$-BODIPY 630/650-X	5.11 ± 0.04	—	—	<5	—	—	>1.2
35	*trans*	$OC(O)C_6H_{12}NH$-BODIPY 630/650-X	No binding	—	—	<5	—	—	—
36	*cis*	$NHC(O)CH_2NH$-BODIPY630/650-X	<5	—	—	<5	—	—	

[a] Radioligand binding performed with [^{3}H]CP55 940 (1 nM) and HEK293-hCB_2 or -hCB_1 membranes. Data is the mean ± SEM of at least three experiments performed in triplicate. Compounds which at 10 μM significantly displaced [^{3}H]CP55 940 but with <50% displacement are annotated as having pK_i >5 M. [b] cAMP levels measured in a BRET assay using a CAMYEL biosensor, in either HEK-293-hCB_2 or hCB_1 cells. Data is the mean ± SEM of at least three independent experiments conducted in duplicate. [c] pIC_{50} calculated by concentration response. [d] E_{max} response (at 10 μM for compounds without pIC_{50} determined. [e] CB_2 receptor selectivity is calculated by: 10^(pK_i CB_2–pK_i CB_1). [f] Except which are two independent experiments performed in duplicate. '—' Indicates that pIC_{50} or E_{max} was not determined. [g] Indicates no significant difference from forskolin only (100%), indicating no measurable response. [h] Except which is at 1 μM due to high non-specific effects at 10 μ, see ESI), normalised to basal (0%) and forskolin only (100%) levels of cAMP. E_{max} >100% is consistent with inverse agonism.

The function of N1-linked naphthyridines **1**, **6** and **8** was analysed using a bioluminescence resonance energy transfer (BRET) biosensor to measure modulation of forskolin-stimulated cyclic adenosine monophosphate (cAMP) at CB_2 and CB_1 receptors (Table 1). All three (**1**, **6**, **8**) were found to increase the level of cAMP, consistent with inverse agonism for CB_2 receptor, in agreement with the literature data for **1** and the reported trend that substitution at the C6 position results in inverse agonism.[25] The most potent for CB_2 receptor was **1**, followed by **8**, while **6** was the least potent. A much lower potency (**6** and **8**) or no response (**1**) was measured for CB_1 receptor. It was concluded from these results (Table 1) that linker and fluorophore substitution at the naphthyridine N1-position is unlikely to lead to fluorescent ligands with useful affinity at CB_2 receptor.

Cyclohexyl-linked naphthyridines. The *cis* isomer showed higher affinity for CB_2 receptor than the analogous *trans* isomer across all cyclohexyl derivatives tested (Table 2), sometimes as much as 1 log unit (**28** *vs.* **29** and **32** *vs.* **33**). This trend is in agreement with *cis*-4-methylcyclohexyl derivatives previously reported to have higher affinity for CB_2 receptor than *trans* analogues.[25,27] There was a dramatic loss in CB_2 receptor affinity for cyclohexanol derivatives **20** and **21** compared to previously reported 1 : 1 *cis*:*trans* methylcyclohexyl **2** (ref. 25) (Table 1) despite the relatively small chemical difference of an alcohol or methyl moiety. The acetylated aminoheptanoate-linked **30** and **31** also showed comparable poor affinity for CB_2 receptor. *Cis*-glycine linked-**28** showed a 0.5 log unit improvement in CB_2 receptor affinity over the analogous *cis*-aminoheptanoate **30**. All cyclohexyl-linked compounds showed little or no affinity for CB_1 receptor.

Amongst all the cyclohexyl-linked naphthyridines, the highest CB_2 receptor affinity (and the only fluorescent ligand with any appreciable affinity) was measured for fluorescent ligand **32** (pK_i = 6.33 ± 0.02 at hCB_2 receptor and >21-fold selectivity over CB_1 receptor). It is interesting that the larger, BODIPY 630/650-contianing **32** showed approximately 0.3 log unit better affinity for CB_2 receptor than the corresponding truncated **28** without the fluorophore (Fig. 2A), implying the BODIPY 630/650 moiety contributed favourably to binding. Similar observations that Class A GPCR fluorescent ligands have higher affinity for the receptor than just the core ligand and/or ligand-linker have also been reported in the literature.[33,34] Despite fluorescent ligand **36** differing from **32** only by replacement of the ester in **32** with an amide, **36** showed minimal binding (pK_i < 5). This could be due to the lack of flexibility of the amide in comparison to the ester, restricting the movement of **36** and preventing favourable positioning of

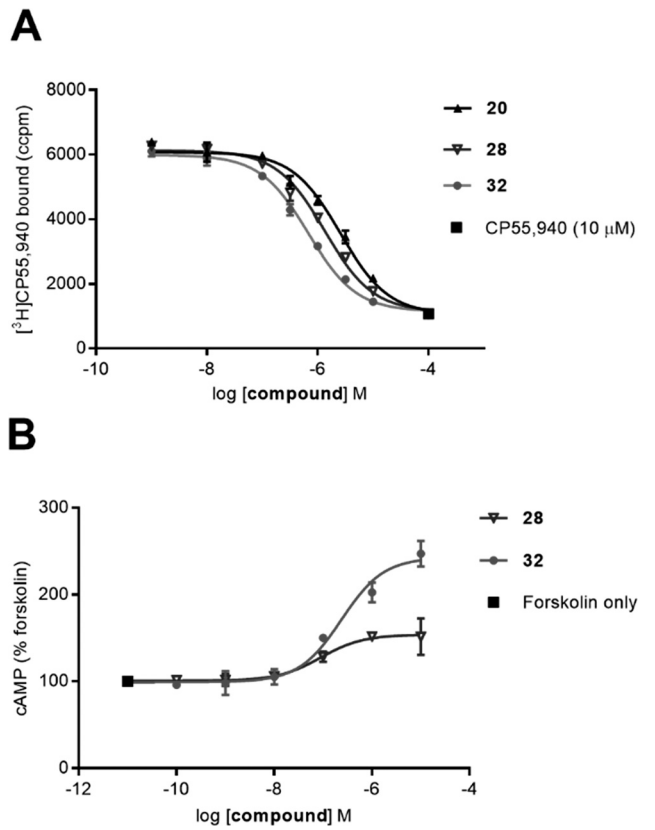

Fig. 2 (A) Competition radioligand binding assay of **20**, **28** and **32** at hCB_2 receptor, using [^{3}H]CP55 940. Data shown is a single experiment conducted in triplicate with error bars showing ±SD; representative of 3 independent experiments. (B) Concentration response curve of **28** and **32** measuring forskolin (5 μM) stimulated cAMP. Area under the curve values from kinetic data were normalised so that forskolin-only response = 100% and basal (vehicle) response = 0%. Representative data from a single experiment conducted in duplicate, with error bars showing ± SD.

the linker and fluorophore relative to the naphthyridine core ligand. However, evaluation of shorter precursors to **36** would be required to draw conclusions.

The ability of cyclohexyl-linked naphthyridines with micromolar or nanomolar affinity for CB_2 receptor to modulate cAMP was determined in a BRET cAMP assay (Table 2). All tested compounds reduced basal signalling (*i.e.* increased cAMP levels) consistent with inverse agonism at CB_2 receptor. The inverse agonist function observed for these cyclohexyl-linked compounds, all which contain a C6-*p*-methoxy benzyl substituent, aligns with literature reports of inverse agonism/antagonism for C6-substituted 1,8-naphthyridin-2(1*H*)-one-3-carboxamides (as also described for compounds in Table 1). The potency of **20**, **28**, **30** and **32** (Fig. 2B shows **28**, **32**) was determined using concentration response assays at CB_2 receptor (and at CB_1 receptor for **32** only). It is interesting that despite **20**, **28** and **32** all having between a 1–1.5 log unit weaker affinity for CB_2 receptor compared to SR144528 (Table 1), **20**, **28**, **32** and SR144528 all showed similar pIC_{50} values at CB_2 receptor. Fluorescent ligand **32** appeared to display a greater E_{max} at CB_2 receptor (hCB_2 pIC_{50} = 6.72 ± 0.18, E_{max} = 210 ± 15.7) compared to SR144528 (hCB_2 pIC_{50} = 6.90 ± 0.08, E_{max} = 153 ± 3.8) and **32** was much less potent at CB_1 receptor (hCB_1 pIC_{50} = 5.26 ± 0.15, E_{max} = 157 ± 2.1). Compounds analysed for potency in the cAMP BRET assay (Tables 1 and 2) were also screened at 10 μM and 1 μM in the parental HEK cells that lack CB receptors (refer to ESI†). A small effect was observed in the parental HEK cells using fluorescent ligand **32** at 10 μM but not at 1 μM (Table S1†). However, due to the low potency of **32** the 10 μM data point of the concentration response assay at CB_2 receptor could not be excluded and therefore the calculated potency of **32** reported at CB_2 receptor is only an estimate. In addition, the higher E_{max} of fluorescent ligand **32** at CB_2 receptor compared to SR144528 could be influenced the small non-receptor mediated effect at 10 μM, thus illustrating the importance of wild type controls to verify receptor-mediated responses.

Ligand **32** is one of the highest affinity CB_2 receptor selective fluorescent ligands reported in the literature to date. It is not possible to meaningfully compare the affinity of **32** to other fluorescent ligands reported in the literature due to different experimental conditions used to measure binding. For example, the affinity of fluorescent ligand 'NIR760-Q' (K_d = 75.5 ± 28.0 nM) was determined in Jurkat cells using a fluorescence saturation binding assay.[20] Fluorescent ligand 'NMP6' had a reported affinity for hCB2 receptor of K_i = 387 nM using CHO-K1 cells, but with no SEM or K_d value provided for the competing radioligand utilised ([^{3}H]CP55 940).[16]

Molecular modelling

The high CB_2 receptor affinity of fluorescent ligand **32** validates the cyclohexyl position as suitable for linker and fluorophore extension. To explore how the ligand-linker of the cyclohexyl-substituted naphthyridines may interact with the receptor, ligand docking studies were performed using a homology model of CB_2 receptor, that was generated using the crystal structure of antagonist bound CB_1 receptor (PDB:5TGZ).[36] To improve docking accuracy, the linker conjugate **28** rather than fluorescent ligand **32** was used. The lowest energy and most consistent docking pose showed the glycine linker of **28** exiting the receptor between TMH1 and TMH7 (Fig. 3A), thus potentially illustrating why the cyclohexyl group is a favourable linker position – allowing an exit point for the linker and fluorophore whilst allowing the core ligand to bind deep within the orthosteric pocket. This is especially interesting in light of previously reported molecular dynamics simulations where a potential ligand entry pathway between TMH1 and TMH7 was identified for anandamide and tetrahydrocannabinol binding to CB_1 receptor,[32] as well as with other fluorescent ligand docking studies at CB_2 receptor.[17,23] The phenyl group of **28** was positioned deep in the hydrophobic region of the binding pocket, in a similar pose to other previously reported docking studies with this naphthyridine scaffold.[25] The methoxy group showed a hydrogen bond with S292, whilst the glycine linker hydrogen

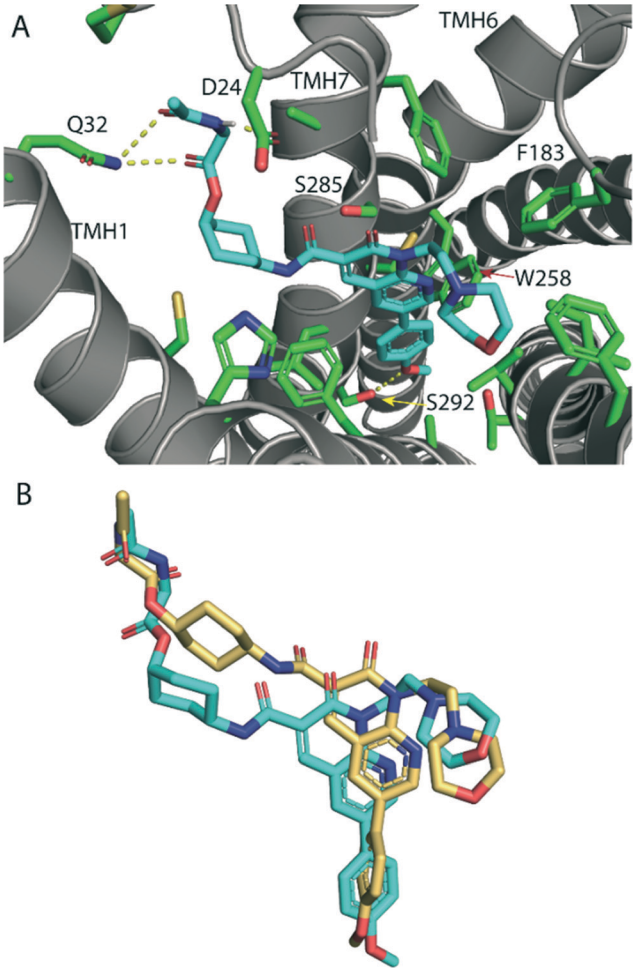

Fig. 3 (A) Lowest energy docking pose of glycine-linked *cis*-**28** (cyan carbon atoms) in hCB_2 receptor homology model (grey ribbons). Hydrogen bonding (yellow dotted line) is shown between the methoxy phenyl oxygen and S292, the ester carbonyl and the glycine amide with Q32 and between the glycine amide and D24. The glycine linker is directed out of the receptor binding pocket between TMH1 and TMH7. Side chains of selected residues within 4 Å of **28** are shown as sticks (green). (B) Overlay of the lowest energy docking poses of *cis*-**28** (cyan) and the analogous *trans*-**29** (gold) docked into hCB_2 receptor homology model (receptor is hidden for clarity), showing that *trans*-**29** is shifted upwards in the binding pocket, which resulted in loss of hydrogen bonding with receptor residues.

bonded with D24 of the amino-terminus and Q32 of TMH1. Favourable placement of hydrogen bond donors and acceptors in the ligand's linker that allow interactions with the polar residues located around the proposed ligand binding pocket entry/exit between TMH1 and TMH7 may be significant for receptor affinity.

The *cis* isomers of the cyclohexyl-linked series consistently showed higher affinities for CB_2 receptor than the *trans* isomers therefore this was explored further through ligand docking studies. In contrast to *cis*-**28**, *trans*-**29** showed an altered pose, in which the whole ligand was shifted upwards in the binding pocket (Fig. 3B). Cyclohexyl-linked *trans*-**29** did not show any hydrogen bonds between the methoxy and S292 or the glycine linker and the residues around the binding pocket exit of TMH1 and TMH7, which may explain the reduced affinity of the *trans* derivatives.

Cellular imaging

Fluorescent ligand **32** showed promise as an imaging tool due to high affinity for CB_2 receptor, selectivity over CB_1 receptor, and a similar pIC_{50} to SR144528. Unfortunately, **32** did not show ideal properties in imaging experiments (Fig. 4). There was little co-localisation of CB_2 receptor (as detected by antibody labelling) with **32**, pre-incubation of cells with a high concentration of non-fluorescent high affinity ligand SR144528 did not appear to prevent or reduce **32** labelling, and application of **32** to cells not transfected with CB_2 receptor still showed a high level of fluorescence. Cell-associated fluorescence arising from **32** was readily detectable within two minutes of incubation, and although fluorescence intensity increased with longer incubation (tested up to 30 minutes) the pattern of staining was equivalent (data not shown). Similarly, incubation with a greater (10 μM) or lesser (1 μM) concentration of **32** influenced the overall intensity of fluorescence but not the subcellular distribution of fluorescence (data not shown). It was concluded that the ester bond of **32** was stable for the duration of the imaging experiments, based on the SAR from **32** and truncated analogues (Table 2, in particular **20** compared to **32**) and from reverse phase high performance liquid chromatography (RP-HPLC) experiments that indicated **32** remained stable with no ester bond cleavage (data not shown). Therefore, reasons for the poor CB_2 receptor imaging properties of **32** are likely due to high levels of membrane association and non-CB_2 receptor associated intracellular accumulation.

Conclusions

A library of 1,8-naphthyridin-2(1*H*)-one-3-carboxamides with linker and fluorophore substitution at the N1 and C3-carboxamide cyclohexyl position were designed, synthesised and pharmacologically evaluated. The N1 position was not tolerant of linker and fluorophore attachment, however a high affinity, selective CB_2 receptor fluorescent inverse agonist (**32**) was developed *via* a C3-carboxamide-cyclohexanol linkage. Despite imaging studies that showed high levels of non-CB_2 receptor-specific fluorescence, **32** remains a promising lead for future fluorescent ligand development because of the affinity and selectivity of this large ligand. Molecular modelling and SAR showed the C3-carboxamide-cyclohexyl position is an excellent position for linker and fluorophore attachment.

Experimental

Chemistry

Chemicals were purchased from Sigma Aldrich, Merck or AK Scientific and BODIPY 630/650-X-OSu from Life Technologies. Anhydrous grade solvents were used when a dry atmosphere was required. Unless stated, all reactions were carried out at

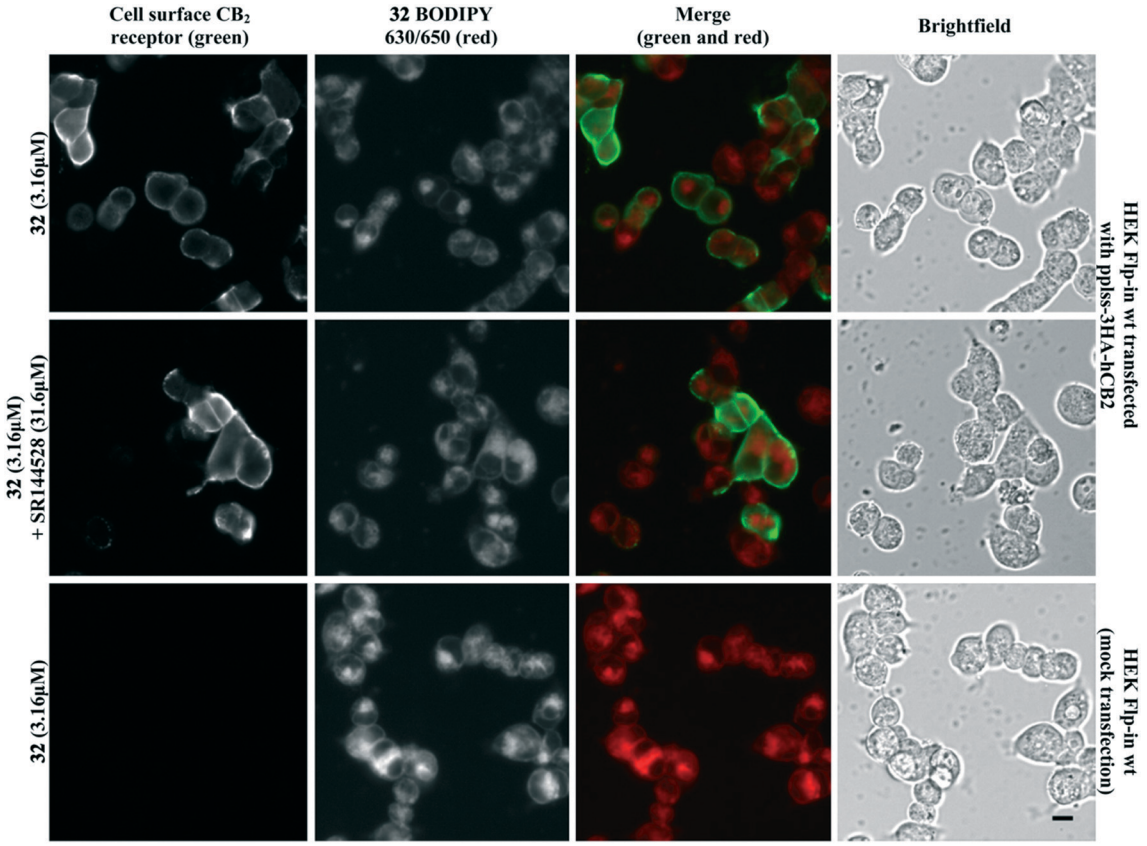

Fig. 4 HEK Flp-in wt cells transiently transfected with pplss-3HA-hCB2 or mock transfection, preincubated with SR144528 or vehicle for 30 min, then treated with **32** + SR144528 or vehicle (2 min followed by 3 washes). Cell surface CB_2 receptor visualised using mouse anti-HA and Alexa 488-conjugated goat anti-mouse. Scale bar 10 μM. Images representative of n = 3 experiments.

room temperature (rt) under atmospheric pressure. Thin layer chromatography was carried out on 0.2 mm aluminium-backed silica gel plates 60 F_{254} and visualised using UV light (λ = 254 nM, 365 nM) and potassium permanganate. Flash column chromatography used 40–63 μm silica. RP-HPLC was carried out on an Agilent 1260 Infinity system with a YMC C8 5 μm (150 × 4.6 mm) or YMC C8 5 μm (150 × 10 mm) column, and mobile phases A: H_2O (0.05% TFA) and B: 9 : 1 acetonitrile (ACN) : H_2O (0.05% TFA). Analytical RP-HPLC retention times were determined using the method −5% B/A 0–1 min, linear gradient of 5–95% B 1–27 min, 95% B 27–28 min, linear gradient of 95–5% B 28–30 min, 5% B/A 30–34 min. All compounds analysed for biological activity were >95% purity by analytical RP-HPLC UV detection at 254, 380 and 550 nm. All compounds HPLC purified as the TFA salt were neutralised using an Amberlyst A21 ion exchange resin before biological testing. High resolution electrospray ionisation mass spectra (HRMS-ESI) were obtained on a microTOF$_Q$ mass spectrometer. Proton and carbon nuclear magnetic resonance (NMR) spectra were obtained on a 400 MHz or a 500 MHz Varian MR spectrometer. Chemical shifts are listed on the δ scale in ppm, spectra are referenced to $CDCl_3$, MeOD-d_4 or DMSO-d_6 residual solvent. Coupling constants (J) are recorded in Hertz (Hz) with signals assigned as: s, singlet; d, doublet; t, triplet; q, quartet; br, broad; or m, multiplet.

Synthesis of fluorescent ligand 32 is detailed below. Synthesis and characterisation of all other compounds is detailed in the ESI.†

6-(4-Methoxyphenyl)-1-[2-(morpholin-4-yl)ethyl]-2-oxo-1,2-dihydro-1,8-naphthyridine-3-carboxylic (19). To a stirred solution of **18** (ref. 25) (6.08 g, 20.5 mmol) in anhydrous DMF (150 mL) was added caesium carbonate (18.67 g, 57.3 mmol). The reaction mixture was stirred for 1 h then 4-(2-chloroethyl)morpholine hydrochloride (7.62 g, 40.1 mmol) was added and the mixture was heated to 50 °C and stirred for 12 h. The DMF was evaporated under reduced pressure and then saturated aq. $NaHCO_3$ (80 mL) was added to the residue, which was then extracted with DCM (3 × 80 mL). The combined organics were washed with H_2O (2 × 80 mL), dried over $MgSO_4$, filtered and evaporated under reduced pressure. Precipitation in ACN yielded a 1 : 3 mixture (5.17 g) of the ethyl ester (ethyl 6-bromo-1-[2-(morpholin-4-yl)ethyl]-2-oxo-1,2-dihydro-1,8-naphthyridine-3-carboxylate) and the carboxylic acid (6-bromo-1-[2-(morpholin-4-yl)ethyl]-2-oxo-1,2-dihydro-1,8-naphthyridine-3-carboxylic acid) as a yellow solid. This 1 : 3 mixture (4.07 g), 4-methoxyphenylboronic acid (2.03 g, 13.3 mmol), Na_2CO_3 (2.83 g, 26.7 mmol) were dissolved in H_2O (25 mL) and DMF (100 mL). $Pd(OAc)_2$ (23 mg, 0.10 mmol) was added and the reaction heated to 110 °C and stirred for 3 h. After cooling to rt, aq. HCl was added

until pH 1–2, H_2O (100 mL) added, and extracted with DCM (3 × 100 mL). The combined organics were washed with H_2O (2 × 150 mL) and sat. aq. NaCl (150 mL), dried over $MgSO_4$, filtered and evaporated under reduced pressure. The residue was washed with EtOH, filtered and the solid dried under reduced pressure yielding a 1 : 15 mixture (1.99 g) of ethyl 6-(4-methoxyphenyl)-1-[2-(morpholin-4-yl)ethyl]-2-oxo-1,2-dihydro-1,8-naphthyridine-3-carboxylate and 6-(4-methoxyphenyl)-1-[2-(morpholin-4-yl)ethyl]-2-oxo-1,2-dihydro-1,8-naphthyridine-3-carboxylic acid, as a yellow solid. A stirred solution of the 1 : 15 mixture (1.9 g) in THF (30 mL) was cooled to 0 °C and 0.2 M LiOH·H_2O (49 mL) was added dropwise. The reaction was stirred at 0 °C for 1 h and then quenched with a biphase of 0.2 M aq. HCl/EA (1 : 1 v:v, 200 mL). The aqueous layer was extracted with DCM (10 × 100 mL), dried over $MgSO_4$, filtered and evaporated under reduced pressure to yield **19** (1.66 g, 4.1 mmol, 20% over three steps) as a yellow solid. ^{1}H NMR (400 MHz, $CDCl_3$) δ 8.97 (d, J = 2.4 Hz, 1H, ArH), 8.93 (s, 1H, ArH), 8.22 (d, J = 2.4 Hz, 1H, ArH), 7.58–7.51 (m, 2H, ArH MeOPh), 7.08–7.01 (m, 2H, ArH MeOPh), 4.86 (t, J = 6.8 Hz, 2H, N1–CH_2), 3.87 (s, 3H, O–CH_3), 3.77–3.64 (m, 4H, O–CH_2 morpholino), 2.93–2.83 (m, 2H, N1–CH_2CH_2), 2.82–2.56 (m, 4H, N–CH_2 morpholino). ^{13}C NMR (101 MHz, $CDCl_3$) δ 164.63, 164.56, 160.41, 152.08, 148.49, 144.86, 135.94, 133.49, 128.33, 128.14, 119.28, 115.08, 115.07, 66.93, 56.00, 55.59, 53.96, 39.37. HRMS-ESI calculated for $C_{22}H_{24}N_3O_5$ $[M + H]^+$ 410.1710, found m/z 410.1701.

***cis*-N-(4-Hydroxycyclohexyl)-6-(4-methoxyphenyl)-1-[2-(morpholin-4-yl)ethyl]-2-oxo-1,2-dihydro-1,8-naphthyridine-3-carboxamide (20).** To a stirred solution of **19** (800 mg, 2.0 mmol) in anhydrous DMF (40 mL) was added DIPEA (1 mL, 5.9 mmol) and HATU (743 mg, 2.0 mmol). The mixture was stirred for 5 min, then *cis*-4-aminocyclohexanol (889 mg, 5.9 mmol) and DIPEA (1 mL, 5.9 mmol) were added and the mixture stirred for 42 h. The reaction mixture was diluted with $NaHCO_3$ (50 mL) and the aqueous phase extracted with DCM (4 × 50 mL). The combined organics were washed with H_2O (2 × 60 mL), dried over $MgSO_4$, filtered and evaporated under reduced pressure. Precipitation in ACN yielded **20** (784 mg, 1.5 mmol, 79%) as a yellow solid. ^{1}H NMR (400 MHz, $CDCl_3$) δ 9.95 (d, J = 7.8 Hz, 1H, NH), 8.91 (s, 1H, ArH), 8.88 (d, J = 2.4 Hz, 1H, ArH), 8.16 (d, J = 2.4 Hz, 1H, ArH), 7.55 (d, J = 8.5 Hz, 2H, ArH MeOPh), 7.04 (d, J = 8.5 Hz, 2H, ArH MeOPh), 4.78 (t, J = 7.1 Hz, 2H, N–CH_2), 4.18–4.08 (m, 1H, CH), 3.96–3.88 (m, 1H, CH), 3.87 (s, 3H, O–CH_3), 3.69 (t, J = 4.6 Hz, 4H, O–CH_2 morpholino), 2.74 (t, J = 7.1 Hz, 2H, N–CH_2), 2.63 (t, J = 4.5 Hz, 4H, N–CH_2 morpholino), 1.94–1.68 (m, 8H, CH_2). ^{13}C NMR (101 MHz, $CDCl_3$) δ 162.56, 162.15, 160.08, 150.57, 148.68, 142.09, 135.40, 132.27, 128.89, 128.24, 123.35, 114.93, 114.77, 67.23, 67.16, 56.04, 55.57, 54.04, 46.58, 39.09, 31.50, 27.64. HRMS-ESI calculated for $C_{28}H_{35}N_4O_5$ $[M + H]^+$ 507.2602, found m/z 507.2552. Analytical RP-HPLC R_t = 14.13 min.

***cis*-4-[6-(4-Methoxyphenyl)-1-[2-(morpholin-4-yl)ethyl]-2-oxo-1,2-dihydro-1,8-naphthyridine-3-amido]cyclohexyl 2-{[(*tert*-butoxy)carbonyl]amino}acetate (23).** A stirred solution of Boc-glycine (17 mg, 99 μmol) and TFFH (26 mg, 99 μmol) in anhydrous DCM (3 mL) was cooled to 0 °C and Et_3N (69 μL, 0.49 mmol) was added. The mixture was warmed to rt and stirred for 30 min and then **20** (50 mg, 99 μmol) and DMAP (1.2 mg, 9.9 μmol) were added. The mixture was stirred for 14 h and then evaporated under reduced pressure. The residue was taken up in EA (3 mL) and washed with H_2O (3 × 3 mL) and sat. aq. NaCl (3 mL), dried over $MgSO_4$, filtered and evaporated under reduced pressure. The residue was purified by flash silica column chromatography (100% EA) to yield **23** (7.4 mg, 11.1 μmol, 19%) as a yellow solid. ^{1}H NMR (400 MHz, $CDCl_3$) δ 9.89 (d, J = 7.7 Hz, 1H, NH), 8.95–8.86 (m, 2H, ArH), 8.17 (d, J = 2.4 Hz, 1H, ArH), 7.62–7.47 (m, 2H, ArH MeOPh), 7.10–6.99 (m, 2H, ArH MeOPh), 5.07–4.99 (m, 2H, NH, CH), 4.80 (t, J = 7.1 Hz, 2H, N1–CH_2), 4.20–4.07 (m, 1H, CH), 3.93 (d, J = 5.7 Hz, 2H, CH_2), 3.88 (s, 3H, O–CH_3), 3.76–3.63 (m, 4H, N–CH_2 morpholino), 2.76 (t, J = 7.1 Hz, 2H, N1–CH_2CH_2), 2.70–2.58 (m, 4H, O–CH_2 morpholino), 1.98–1.71 (m, 8H, CH_2), 1.47 (s, 9H, *t*Bu CH_3). 13C NMR (101 MHz, CDCl3) δ 169.94, 162.61, 162.24, 160.13, 150.68, 148.69, 142.25, 135.45, 132.38, 128.87, 128.27, 123.24, 114.97, 114.79, 80.11, 70.85, 67.18, 56.06, 55.59, 54.07, 46.82, 42.82, 39.17, 28.53, 28.49, 27.74 (one quaternary carbon not observed). HRMS-ESI calculated for $C_{35}H_{46}N_5O_8$ $[M + H]^+$ 664.3341, found 664.3343.

***cis*-4-[6-(4-Methoxyphenyl)-1-[2-(morpholin-4-yl)ethyl]-2-oxo-1,2-dihydro-1,8-naphthyridine-3-amido]cyclohexyl 2-[6-(2-{4-[(*E*)-2-[2,2-difluoro-4-(thiophen-2-yl)-1λ4,3-diaza-2λ4-boratricyclo[7.3.0.03,7]dodeca-1(12),4,6,8,10-pentaen-12-yl]-ethenyl]phenoxy}acetamido)hexanamido]acetate (32).** A solution of **23** (7.0 mg, 10.4 μmol) was dissolved in DCM (0.8 mL) and TFA (0.2 mL) was added. After 1 h stirring, the reaction mixture was evaporated under N_2 stream, followed by reduced pressure. The crude was purified by semi-preparative RP-HPLC to yield the TFA salt *cis*-4-[6-(4-methoxyphenyl)-1-[2-(morpholin-4-yl)ethyl]-2-oxo-1,2-dihydro-1,8-naphthyridine-3-amido]cyclohexyl 2-aminoacetate (4.3 mg, 4.75 μmol, 45%) as a yellow solid. Analytical RP-HPLC R_t = 12.83 min. To a solution this TFA salt (2.8 mg, 3.1 μmol) in anhydrous DMF (500 μL), was added a solution of DIPEA (1.7 μL, 10 μmol) in DMF (128 μL), then BODIPY 630/650-X-OSu (1.25 mg, 1.89 μmol) in DMF (100 μL). The mixture was swirled, left for 12 h, then evaporated under reduced pressure. The crude product was purified by semi-preparative RP-HPLC and passed through an Amberlyst A21 ion exchange resin to yield **32** (2.03 mg, 1.83 μmol, 97%) as a bright blue solid. HRMS-ESI calculated for $C_{59}H_{64}BF_2N_8O_9S$ $[M + H]^+$ 1109.4582, found m/z 1109.4556. Analytical RP-HPLC R_t = 20.47 min.

Pharmacology

Radioligand binding assays. Cell membranes were isolated from HEK (human embryonic kidney) 293 cells (ATCC, Manassas, VA, USA; #CRL-1573) stably transfected with either hCB_1 or hCB_2 receptors[37,38] and binding assays carried out as previously described with minor modifications.[39] Briefly, membranes were resuspended in binding buffer (50 mM

HEPES, 1 mM $MgCl_2$, 1 mM $CaCl_2$, 0.2% [w/v] fatty acid free bovine serum albumin [FAF BSA; MP Biomedicals, Auckland, New Zealand], pH 7.4) to give a final assay concentration of 10 μg per well (Table 1) or 7.5 μg per well (Table 2) for hCB_2 or 7.5 μg per well (Table 1) or 5 μg per well (Table 2) for hCB_1. Compounds (stocks at 10 mM in DMSO, except CP55 940 (Cayman Chemical, Michigan, USA) which was 10 mM in EtOH) were serially diluted using binding buffer containing the requisite amount of EtOH and DMSO to maintain equivalent vehicle levels throughout the dilution series and between all compounds. For vehicle control points, binding buffer containing matched concentrations of EtOH and DMSO was used in place of test ligands. [^{3}H]CP55 940 (PerkinElmer, Waltham, MA, USA) was used at a final concentration of 2.5 nM (Table 1) or 1 nM (Table 2). V-Bottom plates containing hCB_2 or hCB_1 membranes, [^{3}H]CP55 940 and ligand (or CP55 940 or vehicle) were incubated at 30 °C for 1 h prior to harvesting and washing on filter plates (treated with PEI to minimise non-specific binding of the ligand), drying, incubation with scintillation fluid and detection. Binding experiments were performed a minimum of three independent times in technical triplicate. Data was analysed with GraphPad Prism 7 (GraphPad Software, Inc., San Diego, CA, USA) and competition binding curves fit by nonlinear regression using one site competition binding. Dissociation constants (pK_i) of compounds were determined using [^{3}H]CP55 940 K_d = 2 nM (hCB_1) or 3 nM (hCB_2), and are expressed as mean ± standard error of the mean (SEM). In cases where less than 50% displacement of [^{3}H]CP55 940 was observed with 10 μM compound, affinity of the compound was deemed too low to be able to generate an accurate competition binding curve. Therefore, a one sample *t*-test ($P < 0.05$) was used to determine if there was significant difference between displacement in the absence (vehicle normalised to 0%) and presence of compound (with CP55 940 normalised to 100%); if so, the ligand was determined to have a $pK_i < 5$, otherwise it was determined to show no significant binding.

cAMP assays. A BRET assay was carried out to measure forskolin-stimulated cellular cAMP in the appropriate HEK 293 cells transfected with a plasmid that encodes for the cAMP biosensor YFP-Epac-RLuc (CAMYEL) as previously described.[38] Briefly, one or two days prior to transfection, HEK 3HA-hCB_1 pEF4A (same as binding), HEK-Flp HA-hCB_2 pcDNA5/FRT (generated as previously described[40]), HEK wild type (WT) (ATCC, #CRL-1573) or HEK-Flp WT (Invitrogen, Carlsbad, CA, USA) cells, were seeded in 10 cm dishes.

Cells were transfected with 5 μg of pcDNA3L-His-CAMYEL plasmid (ATCC) using 30 μg of linear PEI (molecular weight 25 kDa; Polysciences, Warrington, PA, USA) in 150 mM NaCl. After 24 h, transfected cells were plated in poly-D-lysine (PDL) (0.05 mg mL^{-1} in PBS; Sigma-Aldrich, St Louis, MO, USA) treated 96-well solid white flat bottom polystyrene TC-treated microplates (Corning) at a density of 60–80 000 cells per well in Dulbecco's Modified Eagle's medium (DMEM) supplemented with 10% fetal bovine serum (FBS; New Zealand-origin, Moregate Biotech, Brisbane, Australia). After 16 h, cells were serum-starved in Hank's balanced salt solution (HBSS, Thermo Fisher Scientific, Waltam, MA, USA) containing 1 mg mL^{-1} FAF BSA, pH 7.4 for 30 min. Cells were then treated with 7.5 μM coelenterazine-h (Nanolight Technology, Pinetop, AZ, USA) for 5 min, followed by addition of ligand or matched vehicle in HBSS plus 1 mg mL^{-1} FAF BSA and 5 μM forskolin (Cayman Chemical, Michigan, USA). A LUMIstar plate reader (BMG Labtech, Ortenberg, German) was used to immediately measure emission signals at 37 °C following ligand addition, which were simultaneously detected at 460/25 nM (Renilla luciferase, RLuc) and 535/25 nM (yellow fluorescent protein, YFP). Assays were carried out a minimum of three times (except where stated) in duplicate. Data analysis was performed using GraphPad Prism, with sigmoidal concentration response curves fit by nonlinear regression using values normalised to the vehicle (0%) or forskolin (100%) values for individual experiments. A *t*-test ($P < 0.05$) was used to determine if there was a significant difference in response for compounds at 10 μM in WT HEK cells to determine receptor mediated signalling.

Molecular modelling

The CB_2 receptor homology model was generated using MODELLER 9.15 (ref. 41) using the structure of the antagonist-bound CB_1 receptor (PDB ID: 5TGZ) as a template, based on a modified sequence alignment between hCB_1 and hCB_2 receptors from the T-Coffee server.[42] Three dimensional models of ligands were generated using Avogadro 1.2 (ref. 43) and minimised using the universal force field. Ligand docking was performed using GOLD v5.5 (CCDC Software)[44] centred on Ser285 extending for a distance of up to 15 Å and visualised in PyMOL (The PyMOL Molecular Graphics System, Version 1.8.6.0 Schrödinger, LLC.).

Cellular imaging

HEK Flp-in wt cells were seeded at a density of 30 000 cells per well in PDL treated Nunc™ 96-well black optical-bottom plates (Thermo Fisher Scientific). Approximately 24 h after seeding, cells were transfected with 125 ng per well of pplss-3HA-hCB_2 or empty pcDNA 3.1 (for mock transfected cells) using Lipofectamine® 2000 Transfection Reagent (0.5 μL per well). All drugs and reagents for imaging assays were prepared in HBSS supplemented with 1 mg mL^{-1} BSA. After expressing for 18–24 h, medium was aspirated and cells incubated with mouse monoclonal anti-HA.11 (Clone 16B12, BioLegend, San Diego, CA, USA) diluted 1 : 500, for 30 min at room temperature. Cells were then briefly washed and co-incubated with Alexa Fluor® 488-conjugated goat anti-mouse secondary antibody (Thermo Fisher Scientific) diluted 1 : 300, and 31.6 μM SR144528 (kindly gifted by Roche; Basel, Switzerland) or Vehicle for 30 min at room temperature. Following a brief wash, cells were then treated with 3.16 μM **32** and SR144528 or Vehicle for 2 min, followed by 3 washes. Cells were then imaged using an ImageXpress® Micro XLS Widefield Microscope (Molecular Devices, Sunnyvale, CA, USA) (20× objective).

Conflicts of interest

There are no conflicts to declare.

Acknowledgements

This work was supported by a University of Otago Research Grant, the School of Pharmacy, University of Otago and the Maurice Wilkins Centre for Molecular Biodiscovery. A. C. was supported by a University of Otago Doctoral Scholarship. We thank Christa Macdonald for her technical assistance with pharmacological assay preparations.

References

1 S. Galiegue, S. Mary, J. Marchand, D. Dussossoy, D. Carriere, P. Carayon, M. Bouaboula, D. Shire, G. L. Fur and P. Casellas, Expression of Central and Peripheral Cannabinoid Receptors in Human Immune Tissues and Leukocyte Subpopulations, *Eur. J. Biochem.*, 1995, **232**, 54–61.

2 D.-J. Chen, M. Gao, F.-F. Gao, Q.-X. Su and J. Wu, Brain Cannabinoid Receptor 2: Expression, Function and Modulation, *Nature*, 2017, **38**, 312–316.

3 I. Katona and T. F. Freund, Multiple Functions of Endocannabinoid Signaling in the Brain, *Annu. Rev. Neurosci.*, 2012, **35**, 529–558.

4 M. E. Ferrini, S. Hong, A. Stierle, D. Stierle, N. Stella, K. Roberts and Z. Jaffar, CB_2 Receptors Regulate Natural Killer Cells That Limit Allergic Airway Inflammation in a Murine Model of Asthma, *Allergy*, 2017, **72**, 937–947.

5 C. Turcotte, M.-R. Blanchet, M. Laviolette and N. Flamand, The CB_2 Receptor and Its Role as a Regulator of Inflammation, *Cell. Mol. Life Sci.*, 2016, **73**, 4449–4470.

6 T. Cassano, S. Calcagnini, L. Pace, F. De Marco, A. Romano and S. Gaetani, Cannabinoid Receptor 2 Signaling in Neurodegenerative Disorders: From Pathogenesis to a Promising Therapeutic Target, *Front. Neurosci.*, 2017, **11**, 30.

7 S. Han, L. Thoresen, J.-K. Jung, X. Zhu, J. Thatte, M. Solomon, I. Gaidarov, D. J. Unett, W. H. Yoon, J. Barden, A. Sadeque, A. Usmani, C. Chen, G. Semple, A. J. Grottick, H. Al-Shamma, R. Christopher and R. M. Jones, Discovery of APD371: Identification of a Highly Potent and Selective CB_2 Agonist for the Treatment of Chronic Pain, *ACS Med. Chem. Lett.*, 2017, **8**, 1309–1313.

8 F. Carbone, F. Mach, N. Vuilleumier and F. Montecucco, Cannabinoid Receptor Type 2 Activation in Atherosclerosis and Acute Cardiovascular Diseases, *Curr. Med. Chem.*, 2014, **21**, 4046–4058.

9 A. I. Fraguas-Sánchez, C. Martín-Sabroso and A. I. Torres-Suárez, Insights Into the Effects of the Endocannabinoid System in Cancer: a Review, *Br. J. Pharmacol.*, 2018, **175**, 2566–2580.

10 M. Aghazadeh Tabrizi, P. G. Baraldi, P. A. Borea and K. Varani, Medicinal Chemistry, Pharmacology, and Potential Therapeutic Benefits of Cannabinoid CB_2 Receptor Agonists, *Chem. Rev.*, 2016, **116**, 519–560.

11 A. J. Vernall, S. J. Hill and B. Kellam, The Evolving Small-Molecule Fluorescent-Conjugate Toolbox for Class a GPCRs, *Br. J. Pharmacol.*, 2014, **171**, 1073–1084.

12 R. Lam, A. B. Gondin, M. Canals, B. Kellam, S. J. Briddon, B. Graham and P. J. Scammells, Fluorescently Labeled Morphine Derivatives for Bioimaging Studies, *J. Med. Chem.*, 2018, **61**, 1316–1329.

13 A. Tabor, D. Möller, H. Hübner, J. Kornhuber and P. Gmeiner, Visualization of Ligand-Induced Dopamine D2S and D2L Receptor Internalization by TIRF Microscopy, *Sci. Rep.*, 2017, 1–11.

14 L. A. Stoddart, A. J. Vernall, S. J. Briddon, B. Kellam and S. J. Hill, Direct Visualisation of Internalization of the Adenosine A_3 Receptor and Localization with Arrestin3 Using a Fluorescent Agonist, *Neuropharmacology*, 2015, **98**, 68–77.

15 L. A. Stoddart, L. E. Kilpatrick and S. J. Hill, NanoBRET Approaches to Study Ligand Binding to GPCRs and RTKs, *Trends Pharmacol. Sci.*, 2017, 1–12.

16 R. R. Petrov, M. E. Ferrini, Z. Jaffar, C. M. Thompson, K. Roberts and P. Diaz, Design and Evaluation of a Novel Fluorescent CB_2 Ligand as Probe for Receptor Visualization in Immune Cells, *Bioorg. Med. Chem. Lett.*, 2011, **21**, 5859–5862.

17 L. Martín-Couce, M. Martín-Fontecha, Ó. Palomares, L. Mestre, A. Cordomí, M. Hernangomez, S. Palma, L. Pardo, C. Guaza, M. L. López-Rodríguez and S. Ortega-Gutiérrez, Chemical Probes for the Recognition of Cannabinoid Receptors in Native Systems, *Angew. Chem., Int. Ed.*, 2012, **51**, 6896–6899.

18 M. Sexton, G. Woodruff, E. A. Horne, Y. H. Lin, G. G. Muccioli, M. Bai, E. Stern, D. J. Bornhop and N. Stella, NIR-Mbc94, a Fluorescent Ligand That Binds to Endogenous CB2 Receptors and Is Amenable to High-Throughput Screening, *Chem. Biol.*, 2011, **18**, 563–568.

19 S. Zhang, P. Shao and M. Bai, In Vivo Type 2 Cannabinoid Receptor-Targeted Tumor Optical Imaging Using a Near Infrared Fluorescent Probe, *Bioconjugate Chem.*, 2013, **24**, 1907–1916.

20 Z. Wu, P. Shao, S. Zhang, X. Ling and M. Bai, Molecular Imaging of Human Tumor Cells That Naturally Overexpress Type 2 Cannabinoid Receptors Using a Quinolone-Based Near-Infrared Fluorescent Probe, *J. Biomed. Opt.*, 2014, **19**, 076016–076018.

21 X. Ling, S. Zhang, P. Shao, W. Li, L. Yang, Y. Ding and C. Xu, Novel Near-Infrared Fluorescence Imaging Probe That Preferentially Binds to Cannabinoid Receptors CB_2R Over CB_1R, *Biomaterials*, 2015, **57**, 169–178.

22 A. S. Yates, S. W. Doughty, D. A. Kendall and B. Kellam, Chemical Modification of the Naphthoyl 3-Position of JWH-015: in Search of a Fluorescent Probe to the Cannabinoid CB2 Receptor, *Bioorg. Med. Chem. Lett.*, 2005, **15**, 3758–3762.

23 A. G. Cooper, C. MacDonald, M. Glass, S. Hook, J. D. A. Tyndall and A. J. Vernall, Alkyl Indole-Based Cannabinoid Type 2 Receptor Tools: Exploration of Linker and Fluorophore Attachment, *Eur. J. Med. Chem.*, 2018, **145**, 770–789.

24 M. Soethoudt, S. C. Stolze, M. V. Westphal, L. van Stralen, A. Martella, E. J. van Rooden, W. Guba, Z. V. Varga, H. Deng,

S. I. van Kasteren, U. Grether, A. P. Ijzerman, P. Pacher, E. M. Carreira, H. S. Overkleeft, A. Ioan-Facsinay, L. H. Heitman and M. Van der Stelt, Selective Photoaffinity Probe That Enables Assessment of Cannabinoid CB2 Receptor Expression and Ligand Engagement in Human Cells, *J. Am. Chem. Soc.*, 2018, **140**, 6067–6075.

25 V. Lucchesi, D. P. Hurst, D. M. Shore, S. Bertini, B. M. Ehrmann, M. Allarà, L. Lawrence, A. Ligresti, F. Minutolo, G. Saccomanni, H. Sharir, M. Macchia, V. Di Marzo, M. E. Abood, P. H. Reggio and C. Manera, CB_2-Selective Cannabinoid Receptor Ligands: Synthesis, Pharmacological Evaluation, and Molecular Modeling Investigation of 1,8-Naphthyridin-2(1H)-One-3-Carboxamides, *J. Med. Chem.*, 2014, **57**, 8777–8791.

26 C. Manera, V. Benetti, M. P. Castelli, T. Cavallini, S. Lazzarotti, F. Pibiri, G. Saccomanni, T. Tuccinardi, A. Vannacci, A. Martinelli and P. L. Ferrarini, Design, Synthesis, and Biological Evaluation of New 1,8-Naphthyridin-4(1H)-on-3-Carboxamide and Quinolin-4(1 H)-on-3-Carboxamide Derivatives as CB_2 Selective Agonists, *J. Med. Chem.*, 2006, **49**, 5947–5957.

27 C. Manera, G. Saccomanni, B. Adinolfi, V. Benetti, A. Ligresti, M. G. Cascio, T. Tuccinardi, V. Lucchesi, A. Martinelli, P. Nieri, E. Masini, V. Di Marzo and P. L. Ferrarini, Rational Design, Synthesis, and Pharmacological Properties of New 1,8-Naphthyridin-2(1H)-on-3-Carboxamide Derivatives as Highly Selective Cannabinoid-2 Receptor Agonists, *J. Med. Chem.*, 2009, **52**, 3644–3651.

28 C. Manera, G. Saccomanni, A. M. Malfitano, S. Bertini, F. Castelli, C. Laezza, A. Ligresti, V. Lucchesi, T. Tuccinardi, F. Rizzolio, M. Bifulco, V. Di Marzo, A. Giordano, M. Macchia and A. Martinelli, Rational Design, Synthesis and Anti-Proliferative Properties of New CB_2 Selective Cannabinoid Receptor Ligands: An Investigation of the 1,8-Naphthyridin-2(1H)-One Scaffold, *Eur. J. Med. Chem.*, 2012, **52**, 284–294.

29 C. Manera, A. M. Malfitano, T. Parkkari, V. Lucchesi, S. Carpi, S. Fogli, S. Bertini, C. Laezza, A. Ligresti, G. Saccomanni, J. R. Savinainen, E. Ciaglia, S. Pisanti, P. Gazzerro, V. Di Marzo, P. Nieri, M. Macchia and M. Bifulco, New Quinolone- and 1,8-Naphthyridine-3-Carboxamides as Selective CB2 Receptor Agonists with Anticancer and Immuno–Modulatory Activity, *Eur. J. Med. Chem.*, 2015, **97**, 10–18.

30 T. Kimura, K. Cheng, K. C. Rice and K. Gawrisch, Location, Structure, and Dynamics of the Synthetic Cannabinoid Ligand CP-55,940 in Lipid Bilayers, *Biophys. J.*, 2009, **96**, 4916–4924.

31 D. P. Hurst, A. Grossfield, D. L. Lynch, S. Feller, T. D. Romo, K. Gawrisch, M. C. Pitman and P. H. Reggio, A Lipid Pathway for Ligand Binding Is Necessary for a Cannabinoid G Protein-Coupled Receptor, *J. Biol. Chem.*, 2010, **285**, 17954–17964.

32 J. Jakowiecki and S. Filipek, Hydrophobic Ligand Entry and Exit Pathways of the CB1 Cannabinoid Receptor, *J. Chem. Inf. Model.*, 2016, **56**, 2457–2466.

33 A. J. Vernall, L. A. Stoddart, S. J. Briddon, H. W. Ng, C. A. Laughton, S. W. Doughty, S. J. Hill and B. Kellam, Conversion of a Non-Selective Adenosine Receptor Antagonist Into A3-Selective High Affinity Fluorescent Probes Using Peptide-Based Linkers, *Org. Biomol. Chem.*, 2013, **11**, 5673–5682.

34 A. J. Vernall, L. A. Stoddart, S. J. Briddon, S. J. Hill and B. Kellam, Highly Potent and Selective Fluorescent Antagonists of the Human Adenosine A3 Receptor Based on the 1,2,4-Triazolo[4,3-a]Quinoxalin-1-One Scaffold, *J. Med. Chem.*, 2012, **55**, 1771–1782.

35 Y. Ni and J. Wu, Far-red and near infrared BODIPY dyes: synthesis and applications for fluorescent pH probes and bio-imaging, *Org. Biomol. Chem.*, 2014, **12**, 3774–3791.

36 T. Hua, K. Vemuri, M. Pu, L. Qu, G. W. Han, Y. Wu, S. Zhao, W. Shui, S. Li, A. Korde, R. B. Laprairie, E. L. Stahl, J.-H. Ho, N. Zvonok, H. Zhou, I. Kufareva, B. Wu, Q. Zhao, M. A. Hanson, L. M. Bohn, A. Makriyannis, R. C. Stevens and Z.-J. Liu, Crystal Structure of the Human Cannabinoid Receptor CB1, *Cell*, 2016, **167**, 750–755.e14.

37 N. L. Grimsey, C. E. Goodfellow, M. Dragunow and M. Glass, Cannabinoid Receptor 2 Undergoes Rab5-Mediated Internalization and Recycles via a Rab11-Dependent Pathway, *Biochim. Biophys. Acta, Mol. Cell Res.*, 2011, **1813**, 1554–1560.

38 E. E. Cawston, W. J. Redmond, C. M. Breen, N. L. Grimsey, M. Connor and M. Glass, Real-Time Characterization of Cannabinoid Receptor 1 (CB 1) Allosteric Modulators Reveals Novel Mechanism of Action, *Br. J. Pharmacol.*, 2013, **170**, 893–907.

39 J. M. McPartland, C. MacDonald, M. Young, P. S. Grant, D. P. Furkert and M. Glass, Affinity and Efficacy Studies of Tetrahydrocannabinolic Acid a at Cannabinoid Receptor Types One and Two, *Cannabis Cannabinoid Res.*, 2017, **2**, 87–95.

40 M. Soethoudt, U. Grether, J. U. R. Fingerle, T. W. Grim, F. Fezza, L. de Petrocellis, C. Ullmer, B. R. A. Usler, C. Perret, N. van Gils, D. Finlay, C. MacDonald, A. Chicca, M. D. Gens, J. Stuart, H. de Vries, N. Mastrangelo, L. Xia, G. Alachouzos, M. P. Baggelaar, A. Martella, E. D. Mock, H. Deng, L. H. Heitman, M. Connor, V. Di Marzo, J. U. R. Gertsch, A. H. Lichtman, M. Maccarrone, P. Pacher, M. Glass and M. Van der Stelt, Cannabinoid CB_2 receptor ligand profiling reveals biased signalling and off-target activity, *Nat. Commun.*, 2016, **8**, 1–14.

41 A. Sali and T. L. Blundell, Comparative protein modelling by satisfaction of spatial restraints, *J. Mol. Biol.*, 1993, **234**, 779–815.

42 C. Notredame, D. G. Higgins and J. Heringa, T-Coffee: A Novel Method for Fast and Accurate Multiple Sequence Alignment, *J. Mol. Biol.*, 2000, **302**, 205–217.

43 M. D. Hanwell, D. E. Curtis, D. C. Lonie, T. Vandermeersch, E. Zurek and G. R. Hutchison, Avogadro: An Advanced Semantic Chemical Editor, Visualization, and Analysis Platform, *J. Cheminf.*, 2012, **4**, 17.

44 G. Jones, P. Willett, R. C. Glen, A. R. Leach and R. Taylor, Development and Validation of a Genetic Algorithm for Flexible Docking, *J. Mol. Biol.*, 1997, **267**, 727–748.